International Journal of Aerospace and Lightweight Structures
Vol. 4, No. 3 (2014) 207–215

doi:10.3850/S2010428615100187

NUMERICAL MODELING OF THERMAL FATIGUE CRACK FROM VIEW POINT OF EDDY CURRENT TESTING

Jing Wang[1,*], Noritaka Yusa[1], Mika Kemppainen[2],
Iikka Virkkunen[2] and Hidetoshi Hashizume[1]

[1] *Department of Quantum Science and Energy Engineering, Graduate School of Engineering, Tohoku University, 6-6 Aramaki Aza Aoba, Aoba-Ku, Sendai, Miyagi 980-8579. jingwang8604@gmail.com.*

[2] *Trueflaw Ltd, Tillinmäentie 3, tila A113, 02330 Espoo, Finland.*

This study evaluates the numerical modeling of thermal fatigue crack from the viewpoint of eddy current testing. Four relative small thermal fatigue cracks are artificially introduced into a type 316 stainless steel plate, and their eddy current signals were measured using a differential type plus point probe. Subsequent numerical simulations model each crack as a region with constant width, uniform conductivity and true profile shown by destructive tests. Analyzing the study together with earlier publications indicates that thermal fatigue crack should be modeled as an almost non-conductive region in a general sense, no matter what are frequency, size of crack and base material.

Keywords: Eddy current testing; Numerical modeling; Thermal fatigue crack.

1. Introduction

Eddy current testing (ECT) is one of electromagnetic nondestructive methods. It was initially regarded as kind of qualitative measurement during the inspection of natural cracks, such as stress corrosion crack (SCC), thermal fatigue crack (TFC) et al. On the other hand, ultrasonic testing (UT) is widely used for quantitatively detecting cracks. However performance of UT is inevitably affected by complexity of natural cracks, e.g. fracture surface roughness and so on [Kemppainen and Virkkunen, 2011]. Therefore, enhancement of inspecting natural cracks is demanded by other non-destructive methods. ECT has become a favorable candidate for the aim with the aid of great progress of electromagnetic computational technology

*Corresponding author.

[Auld and Moulder, 1999]. In fact quite a few studies have been reported success in quantitative evaluation of SCC and also they pointed out that modeling of crack is the issue for the accurate measurement [Yusa *et al.*, 2005, 2003], [Badics *et al.*, 1995]. Based on this, modeling of TFC should be emphasized for the accurate eddy current inspection. However, only few studies with relative large TFC have been discussed on the matter [Wang *et al.*, 2013], [Chen *et al.*, 2009]. Further researches by more specimens are needed.

This study was conducted on the basis of the above background to discuss the modeling of relative small TFC from the view point of ECT.

2. Materials and Methods

2.1. *Fabrication of Thermal Fatigue Crack Samples*

One type 316 stainless steel plate was prepared for this study. The plate measured 250 mm long, 150 mm wide and 25 mm thick. Alternate heating by coil and cooling by water spray were loaded so that thermal fatigue cracks were introduced on the surface of plate. Hereafter, these four cracks are denoted as TFC1-4. These artificial TFCs were regarded as favorable representatives of service-induced TFCs according to the previous study [Kemppainen and Virkkunen, 2011].

2.2. *Eddy Current Testing*

Figure 1 shows eddy current testing setup measuring these TFCs. A differential type plus point probe illustrated in Fig. 2 is used. The probe scanned along lines parallel to a crack with lift-off 0.7 mm. Frequencies of 100 kHz, 200 kHz and 400 kHz were used during the inspection respectively. Eddy current signals were all calibrated so

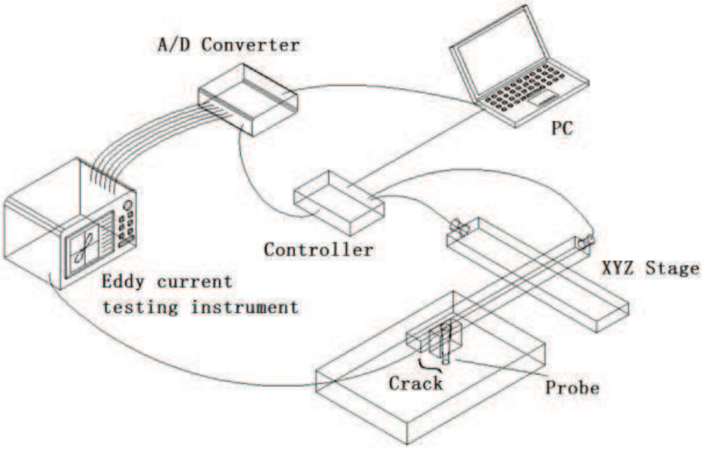

Fig. 1. Eddy current testing setup.

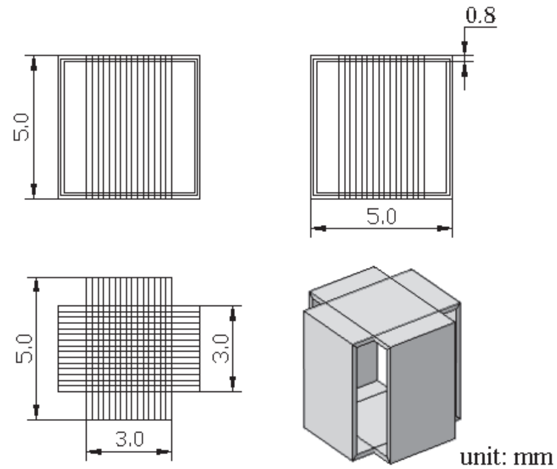

Fig. 2. Plus point probe.

that the maximum signals due to an artificial rectangular slit of 20 mm long, 0.5 mm width and 5 mm deep had amplitude of 10 V and phase of 45 degrees.

2.3. *Destructive Tests*

The specimen was cut into several planes perpendicular to a crack to reveal the true profiles of TFCs after the eddy current testing. Table 1 shows results of destructive tests.

2.4. *Numerical Simulations*

AC/DC module of Comsol Multiphysics 4.4 was used to carry out finite element simulations. The governing equation is

$$(j\omega\sigma - \omega^2\varepsilon)A + \nabla \times (\mu^{-1}\nabla \times A) = J_e \tag{1}$$

where ω is the angular frequency, σ is the conductivity, ε is the permittivity, A is the magnetic vector potential, μ is the permeability and Je is the current density of the exciter. A curl element was utilized in the numerical model.

Table 1. Appendix A. Results of destructive tests

	Max. length (mm)	Max. depth (mm)
TFC-1	9.40	2.06
TFC-2	9.10	2.29
TFC-3	TFC-4	8.50
9.10	2.04	2.11

Figure 3 illustrates geometry of model of numerical simulations. The length and width of plate is sufficient long to avoid edge effect and the thickness of plate is same with that of experiments. TFCs were defined as a region with constant width along the direction of length, uniform conductivity and true profile according to table 1 in the simulations. The width of crack was assumed to be either 0.01 mm, 0.02 mm, 0.05 mm, 0.10 mm or 0.20 mm. The conductivity of crack was set to be either 0.0%, 0.1%, 0.2%, 0.5%, 1.0%, 2.0% or 5.0% of conductivity of base material in order to avoid too many simulations. Simulated eddy current signals were also calibrated after the calculation. Because of the calibration, it is not important to use special current value of probe. Here the current of the probe was supposed to be 1A.

Mesh of the numerical simulation is shown in Fig. 4. Figure on the left side illustrates large region including plate, probe and flaw. The part of plate which is far from probe was roughly meshed for decreasing number of elements. Figure on the right side demonstrates region near probe and flaw. Surface of plate were meshed into several finer layers long the Z direction due to demand on skin depth.

The size of the computational domain was 200 mm × 200 mm × 200 mm. The boundary condition was imposed so that the tangential component of the magnetic vector potential was zero. The total number of elements of the model was about 200,000. Each simulation took about 5 minutes on a PC with Window8-64 bit and RAM 8.0 GB. The mesh was sufficient fine so that error caused by the mesh was only 0.1% of signal. The conductivity and relative permeability were 1.3e6 S/m and 1.0, respectively.

The difference between the measured and simulated signals was evaluated by

$$\varepsilon = \Sigma_{i=1}^{i=5} \left| V_{sim}^{i} - V_{\exp}^{i} \right| \tag{2}$$

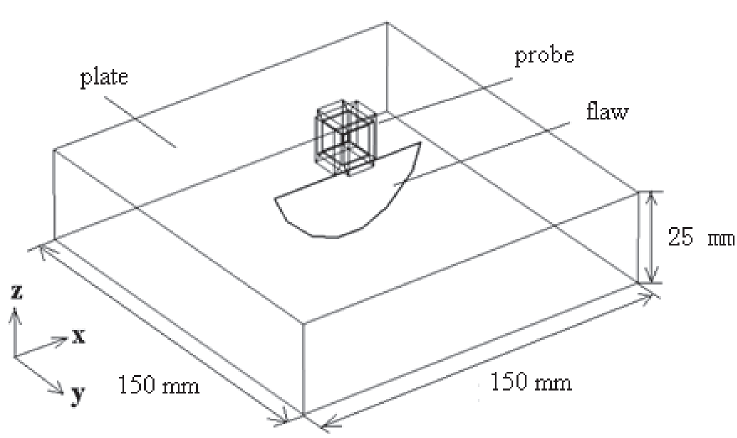

Fig. 3. Geometry of model of numerical simulation.

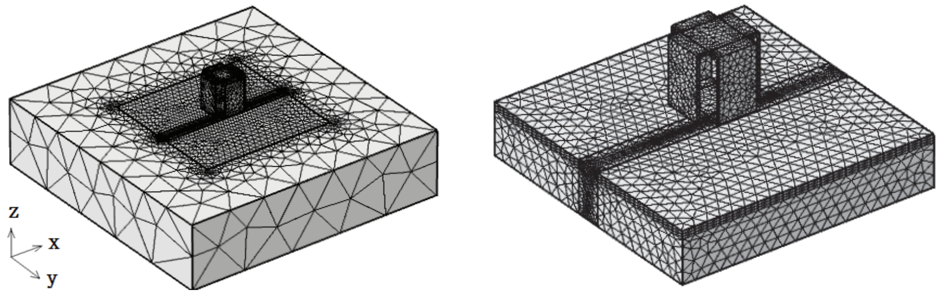

Fig. 4. Mesh of the numerical simulation.

where Vsim and Vexp denote simulated and experimental eddy current signals, i means the i-th scanning points. 5 scanning points directly above the crack are considered to evaluate trajectory. The conductivity and the width minimizing Eq. (2) are defined as the appropriate conductivity and appropriate width.

3. Results and Discussion

Figure 5 shows the change of difference calculated by Eq. (2) in function of conductivity of TFC with frequency of 100 kHz. Results with frequencies of 200 kHz and 400 kHz show similar trend of Fig. 5. Table 2 lists the appropriate width, conductivity and error when the difference of Eq. (2) is smallest, here error is defined by difference of Eq. (2) divided by experimental results. It could be concluded that TFCs in type 316 stainless steel are non-conductive, which is indicated by value of appropriate conductivity. Furthermore, change of frequency does not affect the appropriate conductivity, even though appropriate width is varied. The resistance defined as the appropriate width divided by the appropriate conductivity remains unchanged. Considering previous studies of modeling TFC [Wang *et al.*, 2013, 2013], [Xie et al., 2011, 2012], [Li et al., 2011] which are studying relative large TFCs generated on type 304 stainless steel and Inconel 600 specimens, it is validated that TFC should be modeled as an almost non-conductive region no matter what is the true size of crack and which kind of base material is used.

Figure 6 presents the trajectories of signals due to TFC-1 with three frequencies when crack is modeled by appropriate width and appropriate conductivity. It shows that differences between simulated and experimental results are mainly caused by real parts of signals. Amplitude of simulated signal is smaller than that of experimental signal because maximum depth was roughly estimated since the cross-sectional profiles of crack are revealed only on several planes. Results of other TFCs follow similar trend.

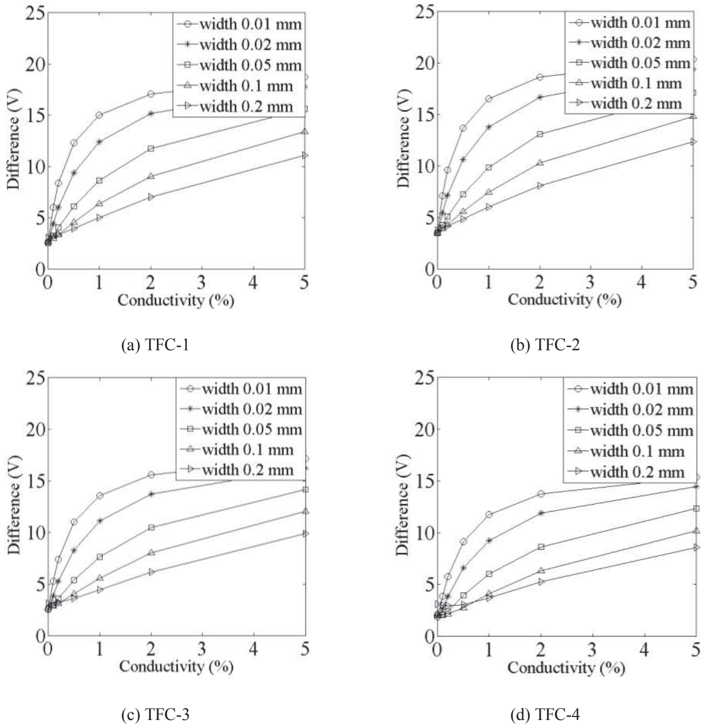

Fig. 5. he relationship between differences calculated by Eq. (2) and conductivity of TFC with frequency of 100 kHz.

Table 2. Appropriate width and conductivity of modeling of TFC.

Flaw ID	Frequency (kHz)	Appropriate width (mm)	Appropriate conductivity (%)	Error
TFC-1	100	0.05	0.0	0.13
	200	0.05	0.0	0.09
	400	0.01	0.0	0.09
TFC-2	100	0.05	0.0	0.16
	200	0.05	0.0	0.14
	400	0.05	0.0	0.14
TFC-3	100	0.02	0.0	0.14
	200	0.02	0.0	0.1
	400	0.01	0.0	0.13
TFC-4	100	0.01	0.0	0.11
	200	0.01	0.0	0.12
	400	0.01	0.0	0.14

Comparison on appropriate conductivities of modeling of SCCs and TFCs are shown as Fig. 7. Those SCCs were investigated in study [Yusa *et al.*, 2007]. They are all evaluated with frequency of 100 kHz. It shows that TFC is almost non-conductive, whereas SCC should be modeled as a region with certain conductivity.

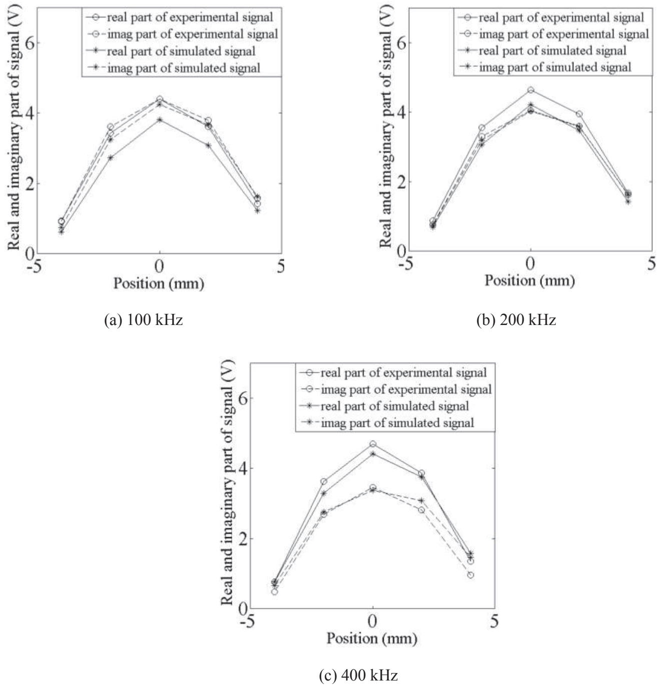

Fig. 6. Trajectories of signals due to TFC-1 with three frequencies.

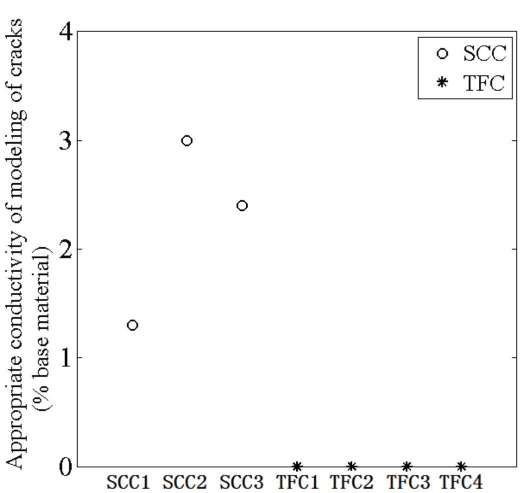

Fig. 7. Comparison on appropriate conductivities of modeling of SCCs and TFCs.

4. Conclusions

This study evaluated numerical modeling of TFC from the aspect of ECT. Four artificial TFCs generated in a type 316 stainless steel plate were prepared for the purpose. Signals were gathered by a differential type plus point probe using several frequencies. TFC was modeled as a region with constant width and uniform conductivity. The appropriate width and conductivity suitable to model the cracks were evaluated based on the measured signals and results of destructive tests. It is revealed that even though the appropriate width varies with change of frequency, the resistance defined as the appropriate width divided by the appropriate conductivity remains unchanged.

Analyzing the results of this study together with those reported in previous publications indicates that TFC should be modeled as an almost nonconductive region regardless of frequency, size of crack and base material. Furthermore, it should be noted that those discussions of modeling TFC are all based on the usage of differential type plus point probe. Therefore, accumulating more data by other types of probes is necessary for the discussion of modeling of TFC on a wider sense.

5. Acknowledgments

This study was conducted as part of the Aging Management Project for System Safety of Nuclear Power Plants commissioned by Nuclear Regulation Authority of Japan.

References

Auld, BA. and Moulder, JC. [1999] "Review of advances in quantitative eddy current nondestructive evaluation," *Journal of Nondestructive Evaluation* **18**(1), 3–36.

Badics, Z., Matsumoto, Y., Aoki, K., Nakayasu, F. and Kurokawa, A. [1995] "Finite element models of stress corrosion cracks (SCC) in 3-D eddy current NDE problem," *Nondestructive testing of materials*. IOS Press.

Chen, Z., Yusa, N. and Miya, K. [2009] "Some Advances in numerical analysis techniques for quantitative electromagnetic nondestructive evaluation," *Non-destructive Testing and Evaluation*, **24**(1–2), 69–102.

Chen, Z., Rebican, M., Miya, K. and Takagi, T. [2005] "3D simulation of remote field ECT by using Ar method and a new formula for signal calculation," *Research in Nondestructive Testing*, **16**, 35–53.

Kemppainen, M. and Virkkunen, I. [2011] "Crack characteristics and their importance to NDE," *Journal of Nondestructive Evaluation* **30**(3), 143–157.

Li, Y., Chen, Z., and Qi, Y. [2011] "Generalized Analytical Expressions of Lift-off Intersection in PEC and a Lift-off-Intersection-based Fast Inverse Model", IEEE Trans. Magn., 47(10), 2931–2934.

Wang, J., Yusa, N., Pan, H. L., Kemppainen, M., Virkkunen, I. and Hashizume, H. [2013] "Discussion on modeling of thermal fatigue cracks in numerical simulation based on eddy current signals," *NDT&E International* **55**, 96–101.

Wang, J., Yusa, N., Pan, H., Kemppainen, M., Virkkunen, I. and Hashizume, H. [2013] "Modeling of thermal fatigue crack for enhancement of electromagnetic nondestructive evaluation of nuclear power plant," *The 21st International Conference on Nuclear Engineering.*

Xie, S., Chen, Z., Takagi T. and Uchimoto T. [2011] "Dvelopment of Efficient Numerical Solver for Simulation of Pulsed Eddy Current Testing Signals", IEEE Trans. Magn., 47, 4582–4591.

Xie, S., Chen, Z., Takagi, T., Uchimoto, T. [2012] "Development of a Very Fast Simulator for Pulsed Eddy Current Testing Signals", NDT&E Int., 51, 45–50.

Yusa, N., Chen, Z. and Miya, K. [2005] "Sizing of stress corrosion cracking on austenitic stainless piping in a nuclear power plant from eddy current NDT signals," *Nondestructive Testing and Evaluation* **20**(2), 103–114.

Yusa, N., Chen, Z., Miya, K., Uchimoto, T. and Takagi, T. [2003] "Large-scale parallel computation for the reconstruction of natural stress corrosion cracks from eddy current testing signals," *NDT&E International* **36**, 449–459.

Yusa, N. Perrin, S. and Miya, K. [2007] "Eddy current data for characterizing less volumetric stress corrosion cracking in nonmagnetic materials," *Materials Letters,* **61**, 827-829.